JET FRAGMENTATION IN $p\bar{p}$ COLLISIONS*

Alexandre Pronko
for CDF Collaboration
University of Florida, Gainesville, FL 32611, USA
e-mail: pronko@fnal.gov

(Received October 6, 2004)

Presented are the latest results on jet fragmentation studies carried out by the CDF Collaboration. Charged particle multiplicities and momentum distributions are measured for quark and gluon jets. The multiplicities are compared to pQCD calculations and earlier results from e^+e^- colliders. Jet shapes for a broad range of jet transverse momenta are measured and compared to Pythia and Herwig Monte Carlo event generator predictions.

PACS numbers: 12.38.Qk, 13.85.Hd, 13.87.Fh

1. Introduction

Jet evolution is driven by multi-gluon emission with very small momentum transfers and is governed by soft QCD. Studying jet fragmentation allows one to perform detailed experimental tests of perturbative QCD. It also facilitates investigation of the border between pQCD and non-pQCD domains. Good understanding of jet fragmentation is important for the success of ambitious high-P_{T} physics programs of Run II at Tevatron and future LHC experiments. Utilizing the differences in quark and gluon jet evolution can be an effective tool for reduction of QCD backgrounds in measurements involving b-jets and/or jets from $W^{\pm} \to q'\bar{q}''$ and $Z \to q\bar{q}$ decays (*e.g.*, $t\bar{t} \to b\bar{b}jjjj$ where the signal is all quark jets and the background is many gluon jets). Many analyses rely on simulation of jets and underlying event by Monte Carlo event generators. Therefore, fragmentation studies in $p\bar{p}$ collisions, which are sensitive to both multi-gluon emissions from the primary final state partons and interactions of proton and anti-proton remnants, provide an important test of underlying event and fragmentation models in Monte Carlo. Finally, jet fragmentation data from the Tevatron complement measurements from e^+e^- and ep experiments, providing a unique test of the universality of jets.

* Presented at the XXXIV International Symposium on Multiparticle Dynamics, Sonoma County, California, USA, July 26–August 1, 2004.

2. Fragmentation of quark and gluon jets

In QCD, quarks and gluons have different coupling strengths for gluon emission expressed by color factors $C_{\mathrm{F}}=4/3$ and $C_{\mathrm{A}}=3$, respectively. It is, therefore, expected that jets produced by quarks and gluons will show differences in their average multiplicity and the shape of momentum spectra of hadrons. Theory views jet fragmentation as a predominantly perturbative QCD process. Analytical predictions are based on the framework of the Modified Leading Log Approximation, MLLA [1], and its various extensions [2, 3], supplemented with the hypothesis of Local Parton–Hadron Duality, LPHD [4].

The CDF results on fragmentation of quark and gluon jets are largely independent of theoretical models of fragmentation. This independence is achieved by exploiting the difference in quark and gluon jet content of dijet events and $\gamma+$ jet events in $p\bar{p}$ collisions. In this measurement, the jets are defined by a cone algorithm with cone radius $R=0.7$ and the energy is corrected to the parton level. Only events with both jets (or γ and jet) in the central region ($|\eta|<0.9$) are retained. The analysis is carried out in the dijet or $\gamma+$ jet center-of-mass frame, where the average jet energies are $E_{\mathrm{jet}}=41$ and 53 GeV. Charged particles are counted in restricted cones with small opening angles $\theta_c=0.28$, 0.36, and 0.47 rad around jet axis, which allows for a direct comparison with theory. The contribution due to underlying event and secondary interactions is subtracted by using a pair of complementary cones defined such that their axis is in the plane normal to the dijet direction and at the same polar angle as the dijet axis. These cones are assumed to collect statistically the same uncorrelated background as the cones around the jets. Assuming gluon and quark jet properties are the same in dijet and $\gamma+$ jet samples, the difference in the fraction of gluon jets ($\sim 60\%$ for dijet and $\sim 20\%$ for $\gamma+$ jet events) in the two samples allows one to algebraically extract the multiplicities in pure quark and gluon jets.

Fig. 1 shows the measured charged particle multiplicities in gluon and quark jets *versus* jet hardness scaling variable $Q=E_{\mathrm{jet}}\theta_c$. Also shown on Fig. 1 are the fits to CDF data obtained by using the recent MLLA expressions from Ref. [3] with normalization constant as the only free parameter (the other parameter Q_{eff} is set to 230 MeV [6]). The width of the bands corresponds to the uncertainty in the overall normalization. The fits for gluon and quark jet data points are independent. One can see that the e^+e^- results [7–9], except for CLEO data points around 5–7 GeV, fall within the fit bands.

The results on the ratio of charged particle multiplicities in gluon and quark jets are presented on Fig. 2. At $Q=19\,\mathrm{GeV}$, the ratio $r=N_g/N_q$ is found to be 1.64 ± 0.17, where statistical and systematic uncertainties are

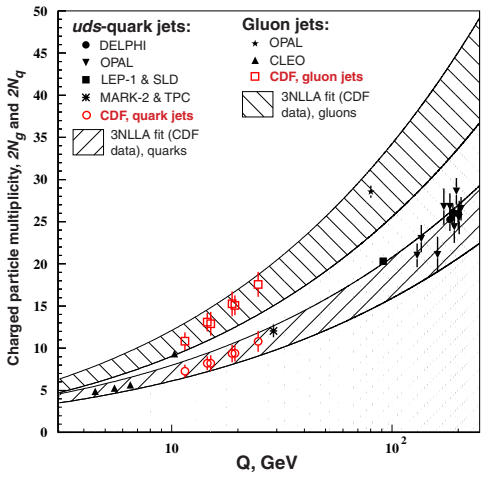

Fig. 1. Average charged particle multiplicities in gluon and quark jets as a function of jet hardness Q, which is $Q = E_{\rm jet}\theta_c$ for CDF data and $Q = E_{\rm c.m.} = 2E_{\rm jet}$ for e^+e^- data.

added in quadrature. The CDF data is found to agree well with re-summed perturbative QCD calculations, $1.4 \leq r \leq 1.8$ [2, 3], and is consistent with recent results from OPAL, $r \simeq 1.5$ [9]. The ratio is also in good agreement with the previous CDF model-dependent measurement, $r = 1.7 \pm 0.3$ [5]. From Fig. 2, one can see that the ratio r tends to increase with energy scale. This trend is statistically significant, because the uncertainties are strongly correlated.

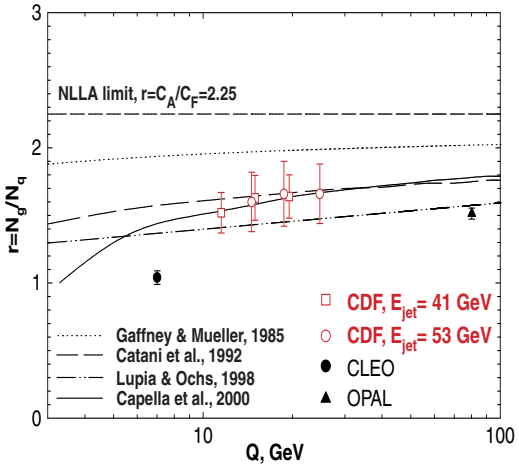

Fig. 2. The ratio of charged particle multiplicities in gluon and quark jets as a function of jet hardness Q. The MLLA curves [2, 3] are calculated using $Q_{\rm eff} = 230\,{\rm MeV}$ [6].

In addition to average multiplicities, we also obtain the momentum distributions, $(1/N_{\rm jet})\,(dN/d\xi)$, of charged particles from gluon and quark jets for $E_{\rm jet} = 41\,\text{GeV}$ and $\theta_c = 0.47\,\text{rad}$. Fig. 3 and Fig. 4 show the comparison of momentum distributions in data with Herwig 5.6 and Pythia 6.115 predictions. As one can see from Fig. 3, both Herwig and Pythia predictions are in a good agreement with the gluon jet data. In case of quark jets (see Fig. 4), both Herwig and Pythia disagree with data significantly leading to $\sim 30\%$ higher charged particle multiplicity than in data. As a result of this difference, both Monte Carlo generators predict significantly lower ratio $r = N_g/N_q$: $r \simeq 1.2$–1.4 compared to $r \simeq 1.5$–1.7 in data.

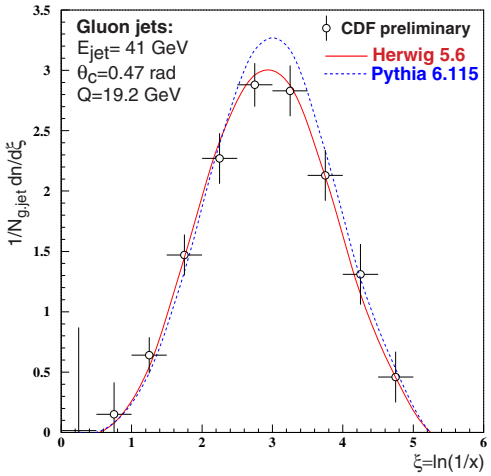

Fig. 3. Inclusive momentum distribution of charged particles in gluon jets.

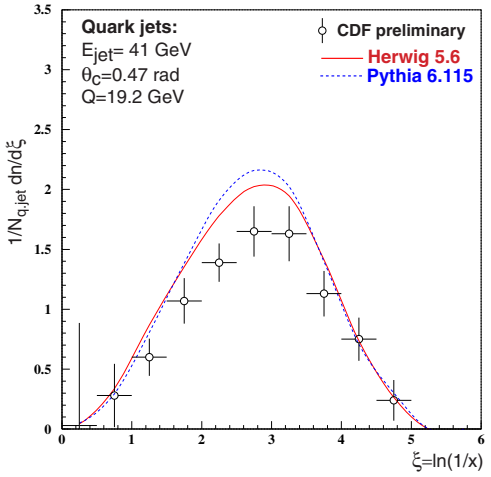

Fig. 4. Inclusive momentum distribution of charged particles in quark jets.

It is also interesting to consider the ratio of momentum distributions, $r(\xi)$, of charged particles from gluon and quark jets. The ratio of multiplicities in gluon and quark jets, r, should approach $r = C_A/C_F = 2.25$ in the asymptotic limit of infinite jet energies. However, this regime can be reached even at current jet energies [10]. For the limited region of phase space, the conservation laws are not a constraint. Thus, the asymptotic condition can be met for soft particles with $p \ll E_{jet}$. The qualitative picture of the effect is that soft gluons have long wavelengths and can not resolve individual partons within a jet. Instead, they only see the color charge of initial parton. Thus, the ratio of mean multiplicities of soft gluons in gluon and quark jets, r_{soft}, should not depend on the energy scale and should approach the asymptotic value of $r_{soft} \to C_A/C_F = 2.25$. As one can see from Fig. 5, the ratio $r(\xi)$ is significantly below unity for energetic particles, and it is monotonously growing as particle momentum gets softer. The ratio appears to saturate at $r_{soft} \simeq 1.8$ which is, however, still below the asymptotic value $C_A/C_F = 2.25$. This difference can be related to the hadronization effects.

The same trends in ratio $r(\xi)$ are also observed in Monte Carlo. Both Herwig and Pythia qualitatively describe the data, but predict somewhat lower ratio in all range of particle momenta. It is also interesting to notice that the OPAL experiment observed the same behavior of $r(\xi)$ and found that the ratio saturates at $r(\xi) \to r_{soft} \simeq 1.8$ (see [9] and Fig. 6).

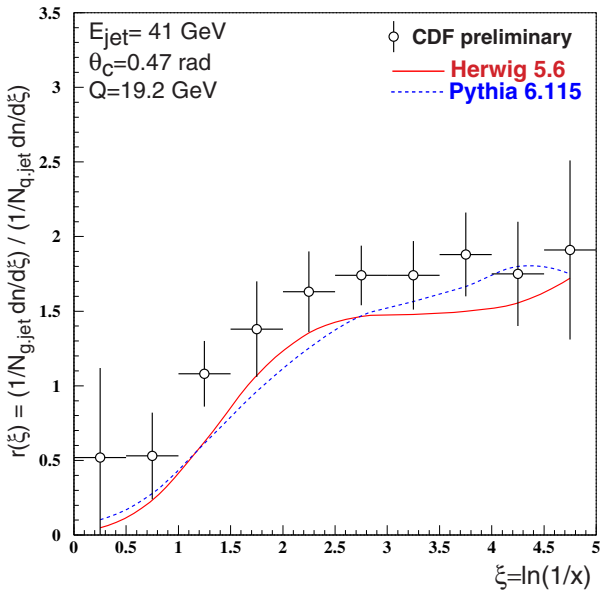

Fig. 5. The ratio of momentum distributions, $r(\xi)$, of charged particles in gluon and quark jets.

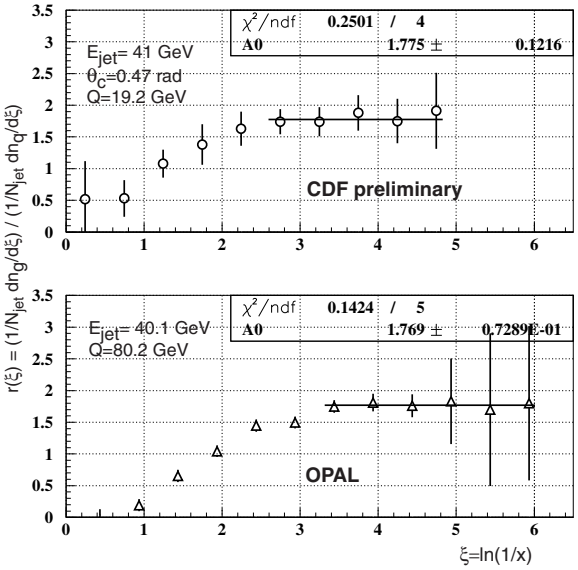

Fig. 6. The ratio of momentum distributions, $r(\xi)$. Comparison of CDF and OPAL.

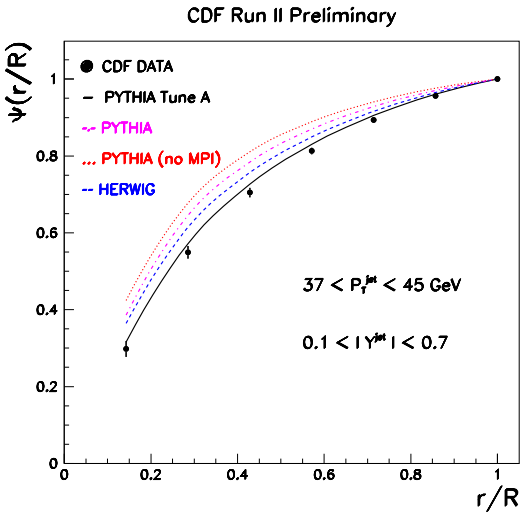

Fig. 7. The measured integral jet shape, $\Psi(r/R)$, in inclusive jet production for jets with $0.1 < |Y^{\rm jet}| < 0.7$ and $37\,{\rm GeV}/c < P_{\rm T}^{\rm jet} < 45\,{\rm GeV}/c$.

3. Jet shapes

The jet shape is a simple measure of how widely a jet's energy is distributed. The integral jet shape is defined as the average fraction of the jet transverse momentum within a cone of a given size r, centered on the jet direction:

$$\Psi(r) = \frac{1}{N_{\rm jet}} \sum_{\rm jets} \frac{P_{\rm T}(0,r)}{P_{\rm T}(0,R)}\,, \qquad 0 \le r \le R\,.$$

The jet shape is dominated by multi-gluon emissions from the primary final-state partons and receives contributions from the soft gluon initial state radiation and interactions of proton and anti-proton remnants. It is also sensitive to the relative fractions of quark and gluon jets in the sample.

The CDF results on jet shapes are based on 170 $\rm pb^{-1}$ of inclusive jet data collected by the CDF experiment in Run II. The measurement is done for central jets, $0.1 < |Y^{\rm jet}| < 0.7$, in the range $37\,{\rm GeV}/c < P_{\rm T}^{\rm jet} < 380\,{\rm GeV}/c$. The jets are reconstructed by the MidPoint algorithm with cone size $R = 0.7$.

The results are compared to the Pythia 6.203 and Herwig 6.4 predictions obtained using the CTEQ5L parton distribution functions. To get deeper insight on the sensitivity of the jet shapes to different components of the underlying event, the data is compared to the Pythia predictions using the default set of parameters with and without the contribution from multi-parton interactions (MPI) between proton and anti-proton remnants, and Tune A [11] set of parameters with the enhanced contributions from the initial state radiation (ISR) and the secondary parton interactions.

Figs. 7, 8 show the measured integral jet shapes for low and high $P_{\rm T}^{\rm jet}$ bins in comparison to the various Monte Carlo predictions. Presented in Fig. 9 is the evolution with $P_{\rm T}^{\rm jet}$ of the average fraction of jet transverse momentum outside of cone $r_0 = 0.3, 1-\Psi(0.3/R)$. From these plots, one can see that jets become narrower as $P_{\rm T}^{\rm jet}$ increases. Pythia-Tune A predictions appear to be in a good agreement with data for entire range of $P_{\rm T}^{\rm jet}$. Herwig gives a good description of the jet shapes for $P_{\rm T}^{\rm jet} > 55\,{\rm GeV}/c$, but produces too narrow jets at lower $P_{\rm T}^{\rm jet}$. It is also interesting to notice that Pythia predictions using the default parameters with and without MPI fail to reproduce data in all range of transverse momenta. The above comparison illustrates the importance of ISR and MPI in a good description of the underlying event.

and merging fraction of 75%. The presented jet shapes are obtained using the calorimeter towers with $P_{\rm T}^{\rm tower} > 0.1\,{\rm GeV}/c$. Fig. 10 shows the evolution of $1 - \Psi(0.3/R)$ with $P_{\rm T}^{\rm jet}$ in comparison to Pythia-Tune A predictions for quark and gluon jets. As one can see, the jets in data look more like gluon jets at low $P_{\rm T}^{\rm jet}$ and more like quark jets at high $P_{\rm T}^{\rm jet}$. This is in agreement with expectations. For a given type of jet in Monte Carlo (quark or gluon), the evolution of $1 - \Psi(0.3/R)$ with $P_{\rm T}^{\rm jet}$ expresses the running of the strong coupling, $\alpha_{\rm s}(P_{\rm T}^{\rm jet})$.

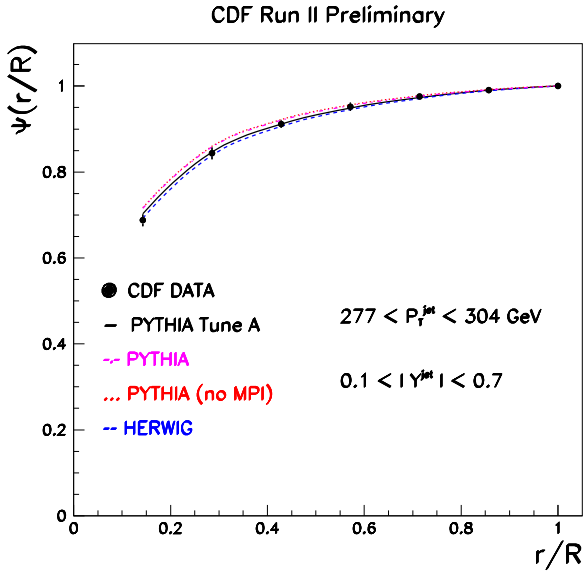

Fig. 8. The measured integral jet shape, $\Psi(r/R)$, in inclusive jet production for jets with $0.1 < |Y^{\rm jet}| < 0.7$ and $277\,{\rm GeV}/c < P_{\rm T}^{\rm jet} < 304\,{\rm GeV}/c$.

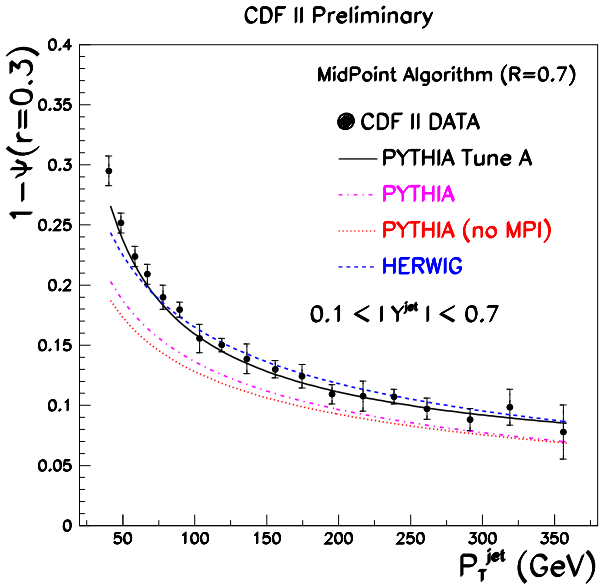

Fig. 9. The measured integral jet shape, $1 - \Psi(0.3/R)$, as function of $P_{\rm T}^{\rm jet}$ in comparison to various Monte Carlo predictions.

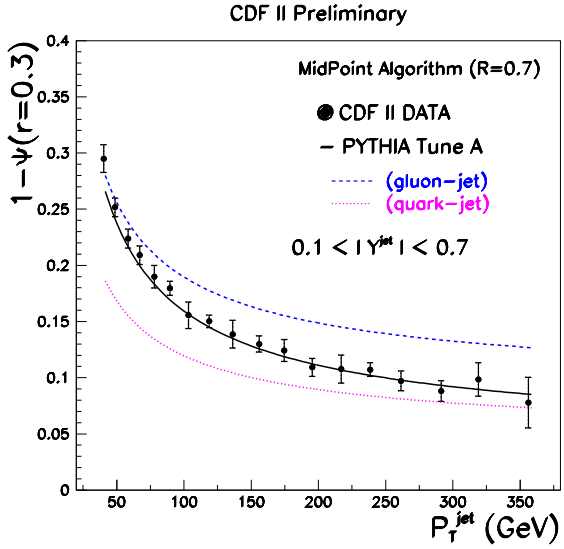

Fig. 10. The measured integral jet shape, $1 - \Psi(0.3/R)$, as function of $P_{\mathrm{T}}^{\mathrm{jet}}$ in comparison to Pythia-Tune A predictions for gluon and quark jets.

4. Conclusion

CDF has measured the average multiplicity and momentum distributions of charged particles in gluon and quark jets. The results are found to agree with re-summed MLLA calculations and are consistent with recent e^+e^- measurements. Herwig 5.6 and Pythia 6.115 reproduce gluon jets fairly well, but over-estimate the multiplicities in quark jets by $\sim 30\%$.

The jet shapes have been measured in inclusive jet production for jets in the kinematic region $37\,\mathrm{GeV}/c < P_{\mathrm{T}}^{\mathrm{jet}} < 380\,\mathrm{GeV}/c$ and $0.1 < |Y^{\mathrm{jet}}| < 0.7$. Pythia-Tune A and Herwig 6.4 predictions are in good agreement with the data for $P_{\mathrm{T}}^{\mathrm{jet}} > 55\,\mathrm{GeV}/c$. The default Pythia 6.203 with and without multi parton interactions of proton and anti-proton remnants fails to describe the jet shapes in all ranges of $P_{\mathrm{T}}^{\mathrm{jet}}$.

REFERENCES

[1] Yu. Dokshitzer, V. Khoze, A. Mueller, S. Troyan, *Basics of Perturbative QCD*, Ed. J. Tran Thanh Van, Editions Frontières, Gif-sur-Yvette 1991.

[2] J.B. Gaffney, A.H. Mueller, *Nucl. Phys.* **B250**, 109 (1985); S. Catani *et al.*, *Nucl. Phys.* **B377**, 445 (1992); S. Lupia, W. Ochs, *Phys. Lett.* **B418**, 214 (1998).

[3] A. Capella *et al.*, *Phys. Rev.* **D61**, 074009 (2000).

[4] Ya.I. Azimov, Yu. Dokshitzer, V. Khoze, S. Troyan, *Z. Phys.* **C27**, 65 (1985); *Z. Phys.* **31**, 213 (1986).

[5] T. Affolder *et al.*, CDF Collaboration, *Phys. Rev. Lett.* **87**, 211804 (2001).

[6] D. Acosta *et al.*, CDF Collaboration, *Phys. Rev.* **D68**, 012003 (2003).

[7] P.C. Rowson *et al.*, Mark II Collaboration, *Phys. Rev. Lett.* **54**, 2580 (1985); H. Aihara *et al.*, TPC Collaboration, *Phys. Lett.* **B184**, 299 (1987); M.S. Alam *et al.*, CLEO Collaboration, *Phys. Rev.* **D46**, 4822 (1992); K. Abe *et al.*, SLD Collaboration, *Phys. Lett.* **B386**, 475 (1996); P. Abreu *et al.*, DELPHI Collaboration, *Eur. Phys. J.* **C6**, 19 (1999); *Phys. Lett.* **B479**, 118 (2000), [Erratum *Phys. Lett.* **492**, 398 (2000)]; K. Ackerstaff *et al.*, OPAL Collaboration, *Eur. Phys. J.* **C1**, 479 (1998); G. Abbiendi *et al.*, *Phys. Lett.* **B550**, 33 (2002).

[8] M.S. Alam *et al.*, CLEO Collaboration, *Phys. Rev.* **D56**, 17 (1997).

[9] G. Abbiendi *et al.*, OPAL Collaboration, *Eur. Phys. J.* **C11**, 217 (1999).

[10] V.A. Khoze, S. Lupia, W. Ochs, *Phys. Lett.* **B386**, 451 (1996); *Eur. Phys. J.* **C5**, 77 (1998).

[11] PARP(67)=4.0, MSTP(82)=4, PARP(82)=2.0, PARP(84)=0.4, PARP(85)=0.9, PARP(86)=0.95, PARP(89)=1800.0, PARP(90)=0.25.